Dynamical Response in Mechanoreceptor on Inner Flagellum of Crayfish to Sinusoidal Wave Train Stimuli

By Kazutoshi KOGA*, Ryoji KATSUBE**, Hidetoshi MIIKE**
and Yoshio EBINA**

(Received July 15, 1980)

Abstract

The swift response of animal to the applied stimuli suggests the importance of phasic characters of firing impulses in the nervous system. Many mechanoreceptors show rapid adaptation and stochastic discharges. To approach the information processing in such receptor system, we examine the dynamic characteristics of mechanoreceptor units on inner flagellum (antennule) of American crayfish (*Procambrus clarkii*). The units were characterized by discharging nerve spikes with different magnitudes. The post-stimulus time histogram (**PSTH**) to sinusoidal wave train (**SWT**) stimuli was studied by a microcomputer measurement system. When a suitable intensity and interval stimulation is applied, we get peculiar **PSTH** which can not be explained by usual exponential function only. In order to understand the behavior of **PSTH** on a unified model, a new idea is proposed on the assumption that firing probability at a period is proportional to the product of normalized recovery function for all previous discharges. The **PSTH** for **SWT** stimuli was well explained with the model. General behaviors of **PSTH** could be understood from the ratio of recovery time constant to the interval between waves of **SWT**.

1. Introduction

Many mechanoreceptors show rapid adaptation for applied mechanical stimuli. It is an interesting problem how much nervous informations are transmitted on parallel fibers in such sensory system. To approach this problem, the dynamic responses are examined. The mechanoreceptor units on the inner flagellum of crayfish have the velocity sensitivity and respond stochastically to the stimulation. The unit is composed of a hair and two cells characterized by discharging high and low amplitude impulses (**HIMP** and **LIMP**), respectively. The impulses fired in respond to the different directional movement of the hair. The authors studied the dynamic responses, post-stimulus-time histogram (**PSTH**), by applying sinusoidal wave train (**SWT**) stimuli. The **SWT** stimuli were used to give two directional stimulations to the hair. The fired impulse trains had different time dependent characters. The time dependency was examined by varying the interval of the stimulus waves and the stimulus intensity. These behaviors of **PSTH** could not be explained by only the adaptation functions which were obtained by conditioning-test stimuli.

The purpose of this paper is to propose a phenomenological model interpreting

* Information Processing Engineering, Technical College
** Department of Electrical Engineering

discharge patterns of **HIMP** and **LIMP** to **SWT** stimuli. The model assumes that the adaptation functions after firing are superimposed successively and determine the later firing condition. This makes a multi-chain of Markoff process. (We call this as a multi-Markoff model). The time course of the adaptation is needed to construct the model. We carry out the experiments of conditioning-test stimuli for our mechano-receptor units. The number of evoked spikes is expressed in probability. Because the origin is not clear yet, the firing probability is considered to be a parameter in this paper.

2. Experimentals

The measurement system is exhibited in Figure 1. Each part is briefly described. **Samples:** The specimens used were inner flagellum of American crayfish (*Procambrus clarkii*) dissected at the protopodite. The proximal cutend of the flagellum was immersed in the van Harreveld solution. The distal portion with sensiella was placed in water so as to mimic the natural environment. This solution was kept constant at about 17°C. The sensory hair (about 100 μm long) was covered with a glass capillary having the tip diameter of 10~20 μm, and stimulated mechanically via the capillary. That was attached on an electro-mechanical transducer (EMT) which was driven by

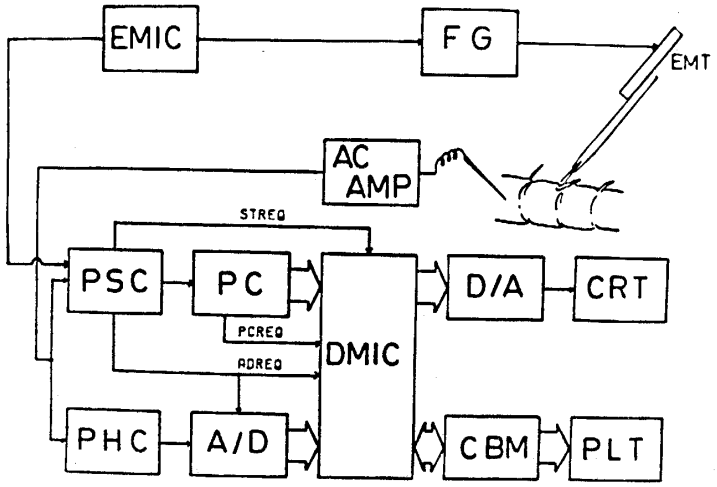

Fig. 1 Block diagram of total measurement system. EMIC gives the initial trigger pulse to FG and PSC. Evoked nerve spikes are amplified by an AC amplifier. EMIC; Microcomputer (Motorola, MEK 6800 D-II), FG; Function generator, EMT; Electro-mechanical transducer, PSC; Pulse sampling circuit, PC; Pulse counter, DMIC; Microcomputer (Motorola, MEK 6800 D-II), PHC; Peak hold circuit, A/D; Analog to digital converter, D/A; Digital to analog converter, CRT; Cathode ray tube, CBM; Microcomputer (Commodore Japan Ltd. CBM 3032,), PLT; X–Y plotter, STREQ; Interrupt request signal informing the end of stimulus, ADREQ; Interrupt request signal informing the start time of amplitude input, PCREQ; Interrupt request signal informing the start time of interval input.

imposing the output voltage from the function generator (FG). The stimulus wave form was the train of the sinusoidal one of 100 Hz as shown in the lowest line in later Fig. 2. This could bend continuously the hair in distal- and proximal-wards from the normal position. The generated nerve impulses were recorded extracellularly with metal electrodes (Insulation; baking enamel, resistance; several MΩ). The responses were observed for the sensory hair bending caused by periodic mechanical stimuli of about 250 msec duration (9 or 10 cycles). The repetition of stimuli was about 500 times with the constant interval of 4 sec.

Computer measurement: The induced impulses were led to the pulse sampling circuit (PSC) and peak hold circuit (PHC). The inter-spike intervals were counted by the pulse counter (PC), and taken into the microcomputer (DMIC). The magnitude of impulse was converted in digital data with analog to digital converter (A/D). The peak values were memorized into DMIC during open of the PSC gate. Simple calculations, such as amplitude histogram, **PSTH** and cycle histogram were conducted on real time utilizing DMIC and monitored on CRT. Furthermore complicated computations were carried out by CBM 3032 microcomputer (345 KByte floppy disk) and final results were hard-copied by X–Y plotter (PLT).

3. Experimental Results

3.1. Response Patterns to SWT Stimuli

Figure 2 is the stereographic histogram displayed on the two-dimensional plane. The histogram was obtained in 0.8 msec time bins. The X axis means the time measured from the start of stimuli. The stimulus waveform is shown below. The Y axis expresses the amplitude of arbitrary unit. The third ordinate stands for the number of impulses. One can observe two impulse trains, high and low ones along Y axis. These were obtained when the PSC gate was open synchronizingly with stimuli. In general, the peak height of **HIMP** was several handreds μV. Noise spikes less than about one half of **LIMP** were excluded. The picture along X axis gives PST histogram for **HIMP** and **LIMP**. Their time courses seem to be different from each other. To see those explicitly, **PSTH**s are rearranged in one dimensional graph. The arising time of **HIMP** and **LIMP** is sharply localized at definite positions of stimulus waves. It can be assumed from our previous observation (Koga, et al., 1980)[1] that **HIMP** discharges at the maximum amplitude and **LIMP** does at the end of stimuli. Thus the time t in **PSTH** is quantized with the period of **SWT** as,

$$t=(n-1)\cdot T, \quad n=1, 2, 3,..., 9, 10 \tag{1}$$

where n means the sequence number of **SWT**. Total number of discharge at each period is counted from the histogram in Figure 2. Typical examples are presented in Figure 3 for several values of the intensity and interval T. The stimulus intensity is expressed by the magnitude of R_∞ (refer to next section). The time course is traced by solid curves connecting experimental values. **HIMP** shows the general tendency

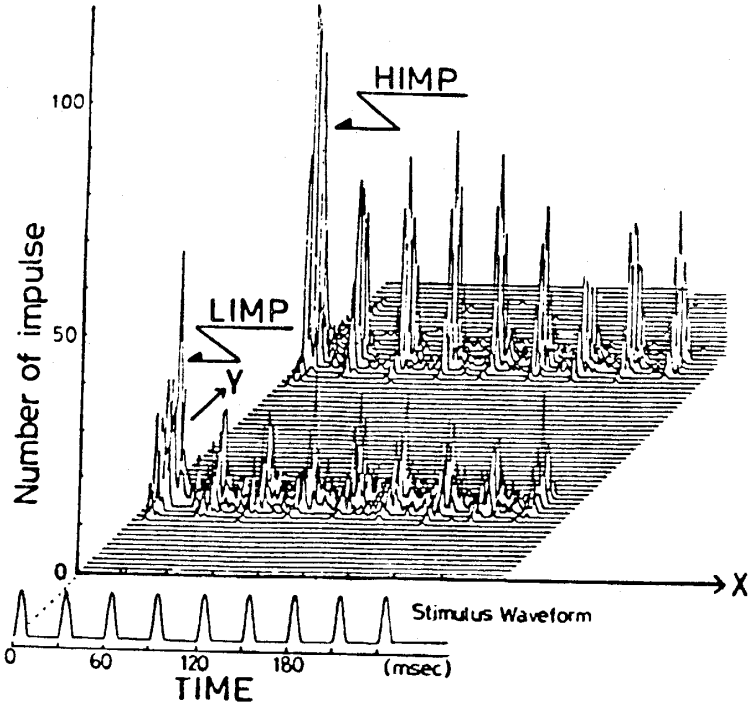

Fig. 2 Amplitude-Post-stimulus time histogram displayed on the two dimensional plane. The lowest waveform is the applied mechanical stimuli of sinusoidal wave train (**SWT**). The upper deflection of **SWT** stands for the bending-down angle of hair from the ordinary position. The abscissa means the time from the starting point of stimuli. The Y axis is the amplitude of arbitrary unit. The repeated times are about 500.

that remarkable changes of firing are seen at 1st, 2nd and 3rd periods and decrease in later phase for large R_∞. In the weak stimuli of $R_\infty \ll 1$, monotonous behaviors are seen. They are the same as those in our previous paper (Kohda, et al., 1978[2]; Koga, et al., 1979[3]). On the other hand, **LIMP** shows steady discharges in the examined range of R_∞.

3.2. The Recovery of Firing Probability after Conditioning Stimuli

The **PSTH** in Figure 3 illustrated the time variant characters of impulses due to dynamic properties of receptor cells. The usual conditioning and test stimulus experiments were conducted. Pairs of sinusoidal mechanical stimuli with equal size were applied repetitively to count the generated impulse numbers. The magnitude of stimuli was adjusted so as to give firing probability less than one in the first cycle. The mean impulse number per stimulus period was obtained by changing the interval T between the first and second stimuli. About 2400 time trials brought the results in Figure 4. The pictures on the first and second lines show those for **HIMP** and **LIMP**, respectively. The value at first cycle is averaged by the number of pair-stimuli. The waveform on the third line is the superposition of paired stimuli (8 times). The spike discharge for test stimuli increases gradually and tends to the value for conditioning

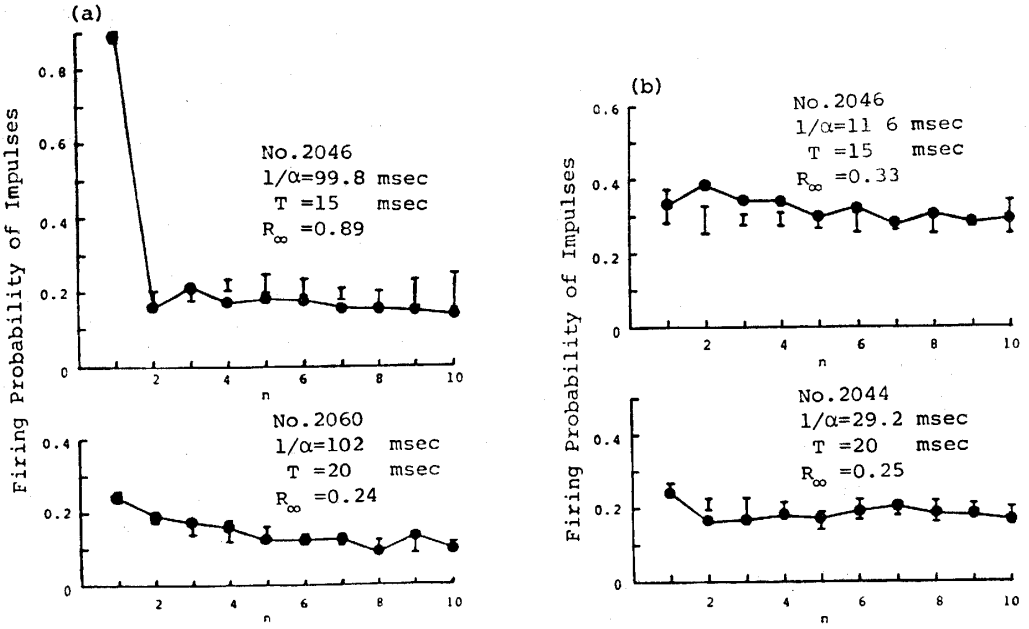

Fig. 3 Rearranged post-stimulus time histogram against the periodical number n of applied **SWT** stimuli. Filled circles are experimental values. Solid curves are drawn by connecting experimental values. The vertical bars indicate the results obtained from multi-Markoff model as shown in 4.1. No.s symbolize the sample number. The recovery time constant $(1/\alpha)$ is the observed value. T is the interval between stimulus waves. The absolute firing probability R_∞ can be seen on the left hand scale. $R_\infty=1$ corresponds to about 0.05 deg. estimated from the extrapolation of calibration curve. 3a; PSTH for HIMP, 3b; PSTH for LIMP.

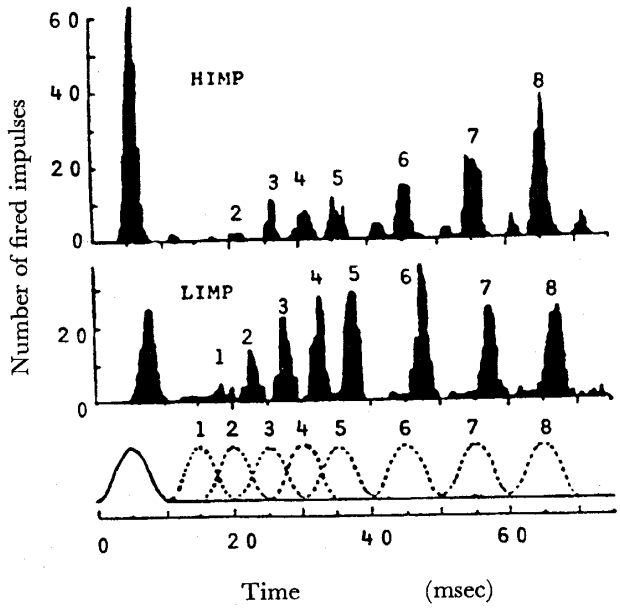

Fig. 4 Post-stimulus time histogram to sinusoidal pair-stimuli. The dotted waves on the third line are the superposition of applied test stimuli. The upper deflection of the waves means the bending-down angle of hair from natural position. PSTH on the first and second lines are for **HIMP** and **LIMP**, respectively.

stimuli with increasing T. The **PSTH** reveals that the recovery speed of **HIMP** is very different from that of **LIMP**.

The **PSTH** for pair-stimuli is expressed as exponential function of first order to construct a stochastic model. Firing position of **LIMP** and **HIMP** was the same as the previous one discussed in 3.1. The firing probability $R(t)$ at t was obtained from the total number of impulses divided by trial times. That at the first cycle is the absolute firing probability (hereafter denoted by R_∞) and similar to the dynamic sensitivity (Thurm, 1965)[4]. The stimulus intensity is roughly proportional to R_∞ (Kohda, et al., 1978)[2]. For later convenience, $R(t)$ is normalized with R_∞, and the symbol $r(t)$ is used. The normalized function $r(t)$ is stimulus-insensitive when the experiments are conducted in the range of $R_\infty \leqq 1$ (Kohda, et al., 1978)[2]. Therefore, $r(t)$ may express the degree of firing regeneration at t after an impulse generation.

Figure 5 presents the average values of $r(t)$ for several samples. Filled circles and squares indicate experimental data for **LIMP** and **HIMP**, respectively. The time course of $r(t)$ is approximated as,

$$r(t)=R(t)/R_\infty=1-\exp(-\alpha(t-\beta)), \qquad (2)$$

where α is the rate constant of firing regeneration or recovery speed constant of firing. The parameter β means the time delay which corresponds to the absolute refractoriness. Two solid curves are drawn by the method of least squares under the presupposed (2) and $\beta=5$ msec. The determined recovery time constant $(1/\alpha)$ is 29 msec for **LIMP** and 104 msec for **HIMP**. The **HIMP** has a longer recovery time constant than **LIMP** and the range is 2.5 to 10 times over samples.

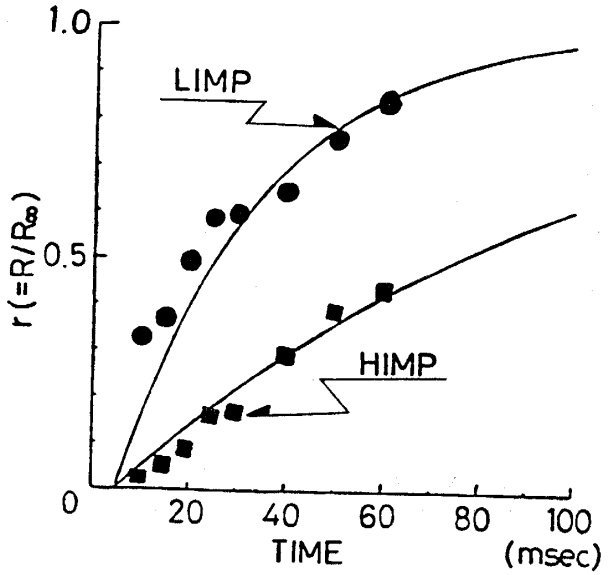

Fig. 5 Time course of normalized firing recovery function for test stimuli. Two solid curves are the exponential functions of the form $[1-\exp(-\alpha(nT-\beta))]$, $\beta=5$ msec and $T=20$ msec. Determined values are $1/\alpha=29$ msec for **LIMP** and 104 msec for **HIMP**. The time is measured from the peaking point of stimulus wave at the first cycle for **HIMP**, and at the end of the stimulus wave for **LIMP**.

4. Interpretation of PSTH by a Multi-Markoff Model

4.1. Simulation with Iterative Calculations

The **PSTH** in Figure 3 illustrated the time variant characters of impulses due to dynamic properties of receptor cells. The impulse generation at sensory neuron evoked some functional changes lasting for several ten milliseconds. In order to disclose this property, we propose a new consideration to construct the firing probability at each cycle. This is a sort of multi-Markoff model.

It is natural that after spike discharges some effects remain in the cell membrane for a while and influence following firing condition. Those are effectively involved in the relative refractoriness. If stimuli are applied within $(1/\alpha)$ and spiking occurs repeatedly, accumulative effects are expected. The accumulation is assumed to be expressed with the product of the functions $r(t)$. When spike discharges at i-th period, $r(t)$ for the spike has the value of $[1-\exp(-\alpha((j-i)T-\beta))]$ at later period j. This is symbolized as

$$r_{ij}=1-\exp(-\alpha((j-i)T-\beta)), \qquad (j>i) \tag{3}$$

where two suffices denote the values between two periods. An example of this process is exhibited graphically in Figure 6. Firing probability at 5-th period $R(5T)_M$ is written down as

$$R(5T)_M=R_\infty \cdot r_{15} \cdot r_{25} \cdot r_{45} \cdot \tag{4}$$

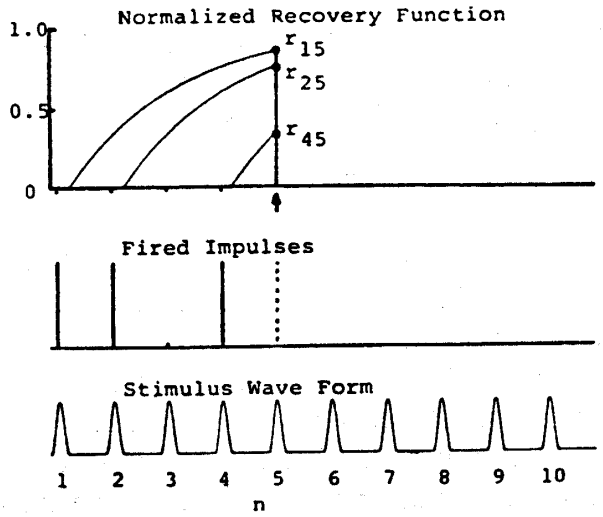

Fig. 6 An example of multi-Markoff process. The wave train on the third line is applied **SWT** stimulation. The vertical bars on the second line indicate supposed firing impulses ($n=1$, 2 and 4). Curves on the third line mean time courses of firing recovery function originating from points of $n=1$, 2 and 4. The firing probability at 5-th period is expressed as $R(5T)_M=R_\infty \cdot r_{15} \cdot r_{25} \cdot r_{45}$, where r_{ij} has the value of $[1-\exp(-\alpha((j-i)T-\beta))]$.

The suffix M emphasizes the one used in Markoff model.

The spikes are not always generated in accordance with stimuli. The stochastic character is simulated with introducing the uniform random number U. The probability whether firing would happen or not is decided as follows:

$$U > R(t)_M \quad \text{no-fire}; \qquad U \leqq R(t)_M \quad \text{fire}, \tag{5}$$

where the condition $0 < R_\infty \leqq 1$ is presumed and U has the range of [0, 1].

Spike discharges for **SWT** stimuli occur at discrete times as (1). To follow the experimentals, iterative computations were firstly carried out with the similar method to that in our previous paper. Utilizing (1), (2), (4) and (5), impulse trains were computed as the average of 500 times calculations. The computation was repeated 10 times to see the range of scattering. There were obtained 10 different values. Typical examples of simulations are also plotted by vertical bars in Figure 3. The length of bar shows the scattered range of ten values. All parameters are decided according to experimental data of pair-stimuli. They coincide well with the experimental values.

4.2. Calculations by Conditional Probability

The iterative computation in the previous section was limited in finite trials. The calculated values were rather scattered in every repetition times. Our interest is to know final **PSTH** after infinitely iterative calculations and behaviors for wide range of R_∞. As a mathematical problem this is equivalent to obtain expectation of firing probability at each stimulus period. Our case is an example of conditional probability ones. The firing probability is assumed to be determined from multi-Markoff model such as (4).

Event starts from $n=1$. Its firing probability is R_∞, and no-firing one is $1-R_\infty$. The probability of complementary event is denoted with an upper bar, as $\overline{R_\infty}(=1-R_\infty)$. In the second period ($n=2$), the case is divided into four ones. The expectation is

$$R_\infty \cdot R_\infty \cdot r_{12} + \overline{R_\infty} \cdot R_\infty, \quad \text{at} \quad n=2.$$

We have 2^k cases in k-th period. The formulas can be easily written down but become long ones. So, some results up to $n=4$ are tabulated in Table 1. Expectations are numerically computed for several combinations of R_∞, T and α. Results for $T=$ 20 msec; $1/\alpha=100$ msec and $T=20$ msec; $1/\alpha=30$ msec are expressed with small filled circles in Figures 7a and 7b. Figure 7a shows **PSTH** for the case of $(1/\alpha)=100$ msec. The curves illustrate the characteristics for **HIMP**. At very small R_∞, they are monotonic. With increasing stimulus intensity or R_∞ the initial peak increases sharply and the dip at the second period appears. The increment at later periods is not so clear as the increment of stimulus intensity. A broad peak is found in large R_∞. These simulate widely **PSTH** for **HIMP** in Figure 3a. Examples of short time constant are seen in Figure 7b. The curves show monotonous behaviors except very large R_∞. At $R_\infty=1$, an initial large peak and following variant discharges are found. The steady discharge at later periods is virtually proportional to the magnitude of R_∞. The curves

Table 1. Conditional probabilities up to 4th period. Attached bars indicate probabilities of corresponding complementary events, such as $\overline{R_\infty \cdot r_{ij}} = 1 - R_\infty \cdot r_{ij}$. n stands for the sequence number of periodical cycle.

$n=1$	$n=2$	$n=3$	$n=4$
R_∞	$R_\infty \cdot r_{12}$	$R_\infty \cdot r_{13} \cdot r_{23}$	$R_\infty \cdot r_{14} \cdot r_{24} \cdot r_{34}$
			$\overline{R_\infty \cdot r_{14} \cdot r_{24} \cdot r_{34}}$
		$\overline{R_\infty \cdot r_{13} \cdot r_{23}}$	$R_\infty \cdot r_{14} \cdot r_{24}$
			$\overline{R_\infty \cdot r_{14} \cdot r_{24}}$
	$\overline{R_\infty \cdot r_{12}}$	$R_\infty \cdot r_{13}$	$R_\infty \cdot r_{14} \cdot r_{34}$
			$\overline{R_\infty \cdot r_{14} \cdot r_{34}}$
		$\overline{R_\infty \cdot r_{13}}$	$R_\infty \cdot r_{14}$
			$\overline{R_\infty \cdot r_{14}}$
$\overline{R_\infty}$	R_∞	$R_\infty \cdot r_{23}$	$R_\infty \cdot r_{24} \cdot r_{34}$
			$\overline{R_\infty \cdot r_{24} \cdot r_{34}}$
		$\overline{R_\infty \cdot r_{23}}$	$R_\infty \cdot r_{24}$
			$\overline{R_\infty \cdot r_{24}}$
	$\overline{R_\infty}$	R_∞	$R_\infty \cdot r_{34}$
			$\overline{R_\infty \cdot r_{34}}$
		$\overline{R_\infty}$	R_∞
			$\overline{R_\infty}$

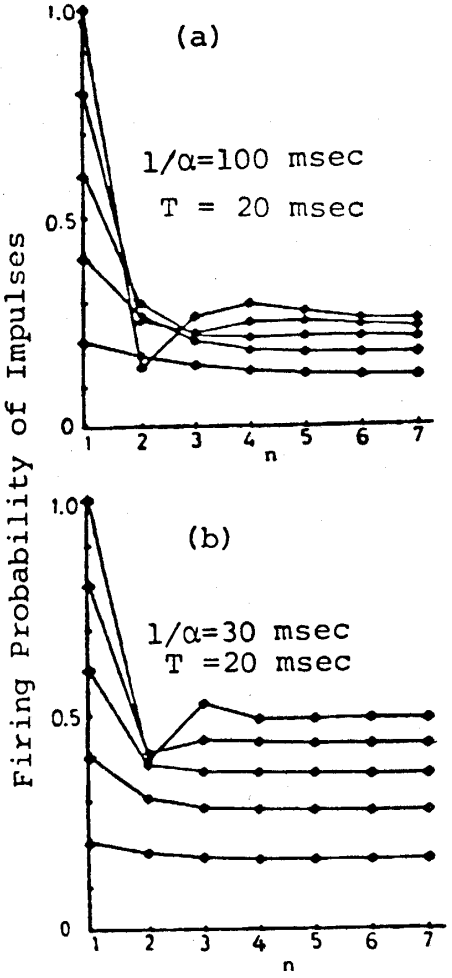

Fig. 7 Post-stimulus time histogram against periodic cycle times. Calculation is carried out by using conditional probabilities, a portion of which is presented in Table 1. Solid small circles are computed values. The absolute firing probability R_∞ are taken to be 1.0, 0.8, 0.6, 0.4 and 0.2, as seen on the left hand scale ($n=1$). n stands for the sequence number of periodical cycle. 7a; PSTH for $1/\alpha=100$ msec, 7b; PSTH for $1/\alpha=30$ msec.

have all the aspects of **PSTH** for **LIMP** found in Figure 3b, although that of $R_\infty=1$ was not observed experimentally yet.

Obtained **PSTH** can be understood from the ratio of $(1/\alpha)$ to T. The ratio is greater than 1, we have phasic character at immediately after applied stimuli and gradual changes of discharged spikes. When the ratio is less than 1, steady discharge patterns are expected, because the firing probability reaches R_∞ at every stimulus time T.

5. Discussions

Dynamic characteristics of **PSTH** were well illustrated on the basis of proposed stochastic model. Mathematical interpretation about it is tried. There were assumed accumulative properties of our nerve cells, although the direct verification has not been performed so far. Significant amount of effect may remain when repetitive firings are attained. Even there is any accumulative effect, the firing probability should be less than R_∞. Another condition is that all $r(t)$ should take part in the event if all previous discharges influence later spike generation. Thus the product as (4) was reasonably proposed.

The **SWT** stimuli had the feature that mechanical stimuli with short duration were intermittently applied. This had similar characters as continuous sinusoidal stimuli (Görner, 1965[5]; Talbot, et al., 1968[6]; Chichibu, et al., 1978[7),8]; Tautz, 1979[9]). Because the interval T could be varied in its wide range, our method was suitable for investigating stimulus dependent properties. The wave form of single frequency in mechanical stimuli was optically verified to hold if the applied frequency was less than 200 Hz (Kohda, et al., 1978)[2]. The cycle histogram behaved in the same manner as that in mechanoreceptors of Monkey hand for flatter stimuli (Talbot, et al., 1968)[6]. With increasing the intensity of stimuli, the firing position moved to a little earlier one together with sharpening the width and higher peaking (Kohda, et al., 1978)[2].

Our previous fatigue model could also simulate **PSTH** found in Figure 3, if the fatigue factor was taken to be different values for **LIMP** and **HIMP** (unpublished data). However, that had some difficulties. The reason of the difference was not clear. And the model assumed that the firing recovery became slow after the generation of spikes due to fatigue of receptor cells. The idea was too intuitive. In the present model, such fatigue factor was not included.

From previous findings we suppose the mechanoreceptor working. We got **PSTH** of one hair from summing up many time trials. This time average is expected to be equivalent as an ensemble average of many hairs because there are many sensory units on the antennule and they are projected to interneurons. If this guess is permitted, the informations obtained by adding several hundred times on a single sensory hair are transmitted secondary neurons as inputs by parallel signal transmissions. The **PSTH** in Figure 7a shows large initial phasic change and small one at steady discharge phase. The peak R_∞ was roughly proportional to the stimulus intensity. On the other hand, **PSTH** in Figure 7b varied with the magnitude of R_∞ in later phase. The initial phasic discharge of **HIMP** may be important for transmitting rapidly informations of movement objects. The **LIMP** is proper for the intensity at rather steady phase of movement such as sinusoidal one (Tautz, 1979)[9]. Furthermore **HIMP** and **LIMP** fire differently in respond to the proximal and distal movements of hair. The discharge patterns being sent on parallel fibers are different from those in electrical engineering devices composed of simple push-pull elements. Thus our sensory system is considered to be an interesting composite one.

Acknowledgements

In course of this study, the authors are grateful to many students who helped the experiments, and to Sokichi Tanito who kindly made several instruments.

References

1) Koga, K., Katsube, R., Miike, H. and Ebina, Y.: An analysis of response characteristics of two mechanoreceptor units on the inner flagellum of American crayfish to sinusoidal wave stimuli by using microcomputer system. Trans. IECE Japan, **63–A**, (to be published) (1980).
2) Kohda, M., Miike, H., Koga, K. and Ebina, Y.: The response of mechanoreceptor units in isolated crayfish antenna to sinusoidal wave stimulation and its probability model. Technical Report, IECE Japan, **MBE 78–52**, 63–71 (1978).
3) Koga, K., Kohda, M., Miike, H., Ebina, Y. and Chichibu, S.: The response of mechanoreceptor units in isolated crayfish antenna to sin-wave stimulation and its probability model. Trans. IECE Japan, **62–C**, 17–23 (1979).
4) Thurm, U.: An insect mechanoreceptor part II: Receptor potentials. In: Symposia on Quantitative Biology. **XXX**, 83–94 (1965).
5) Görner, P.: A proposed transducting mechanism for a multiply-innervated mechanoreceptor in spiders. In: Symposia on Quantitative Biology, **XXX**, 69–73 (1965).
6) Talbot, W. H., Smith, I. K., Kornhuber, H. H., Mountcastle, V. B.: The sense of flutter vibration comparison of the human capacity with response patterns of mechanoreceptive afferents from the monky hand. J. Neurophysiol. **31**, 301–334 (1968).
7) Chichibu, S.: Activities of velocity-sensitive mechanoreceptor in the crayfish. Acta medica Kinki Univ. **3**, 167–175 (1978).
8) Chichibu, S., Tani, Y. and Tsukada, M.: Sinusoidal mechanical stimulation and the frequency characteristics of the crayfish setal neurons. Acta medica Kinki Univ. **3**, 191–201 (1978).
9) Tautz, J.: Response of particle oscillation in a medium unorthodox sensory capacity. Naturwissenshaften, **66**, 452–461 (1979).